Journal of Orthopaedics 15 (2018) 138–142

Contents lists available at ScienceDirect

Journal of Orthopaedics

journal homepage: www.elsevier.com/locate/jor

Bizarre parosteal osteochondromatous proliferation: 16 Cases with a focus on histologic variability

Margaret Cocks[a,1], Elizabeth Helmke[a,1], Carolyn A. Meyers[a], Laura Fayad[b], Edward McCarthy[a], Aaron W. James[a,*]

[a] Department of Pathology, Johns Hopkins University, United States
[b] Department of Radiology, Johns Hopkins University, United States

ARTICLE INFO

Keywords:
BPOP
Bone tumor
Cartilage tumor
Osteochondroma
Surface bone tumor

ABSTRACT

Bizarre parosteal osteochondromatous proliferation (BPOP) is a benign bone and cartilage forming tumor occurring on the surface of bones, predominantly on the hands and feet. A defining feature of BPOP is the purplish-blue mineralization of cartilaginous tissue, known as 'blue bone.' Here, we report on an institutional series of 16 cases of BPOP, including radiographic, histologic, and histomorphometric features. All tumors were composed of some element of bone, cartilage, fibrous tissue and 'blue bone,' though the amount of each tissue sub-type varied widely. Some cases showed focal 'blue bone' only, however this was a defining feature in all cases.

1. Introduction

Bizarre parosteal osteochondromatous proliferation (BPOP, also called Nora's Lesion) is a benign tumor that occurs predominantly in the tubular bones of the hands and feet including the phalanges, metacarpal and metatarsal bones.[1,2] BPOP may occasionally arise on the long bones. BPOP has been found in patients ranging in age from 8 to 73 years, though the tumor is most common during the second and third decades.[1] No sex predilection has been identified. Tumors generally are less than 3 cm and are painless. A history of trauma is elicited in about 10% of cases. Recurrence is common and may be seen in up to 50% of cases, likely due to partial excision. On radiographic imaging, BPOP is most often described as a well-circumscribed, radiodense mass arising adjacent to the cortical surface.[1,2] Medullary continuity between the lesion and native bone is not seen.

Grossly, the appearance of BPOP is that of a bone and cartilage containing exophytic mass without continuity with the underlying bone medullary cavity. BPOP tumors may be received intact or as a morselized tissue aggregate. Histologically, BPOP has a 'disorganized' architectural appearance on low magnification, with aggregates of cartilage, new bone, and fibrous tissue. In some cases, a cartilaginous cap may be seen. BPOP is often marked by hypercellular, reactive and somewhat atypical cartilage and fibrous stroma, which invokes concern over the lesion's malignant potential. Marked nuclear hyperchromasia or atypical mitotic figures are not seen. A distinguishing feature of BPOP is blue-staining osteocartilaginous tissue, known as 'blue bone.'

As BPOP is a rare and frequently misdiagnosed tumor, we reviewed our institutional case files for all observed cases. Sixteen cases of BPOP were identified with radiographic and histologic correlates, which shed new light on both the common features and variability within this unusual entity.

2. Methods

2.1. Identification of bizarre parosteal osteochondromatous proliferation samples

Sixteen cases diagnosed as BPOP were identified in our surgical pathology archives (dated 1994–2016). IRB approval was obtained, which included a waiver of informed consent for this retrospective case series. The clinical, radiographic, and histologic data of the sixteen cases were compiled. Two pathologists independently verified the diagnoses.

2.2. Image acquisition

Radiographic images were obtained from institutional case files, imaged using a 12-megapixel digital camera with an f/2.2 aperture (Fig. 1). Histological slides were digitally scanned using an Aperio automated slide scanner, and one representative image of each sample was taken. Additional images for publication were taken using the NDP view2 software at 40 x and 100 x magnification (Fig. 2).

* Corresponding author at: Department of Pathology, Johns Hopkins University, Ross Research Building, Room 524A,720 Rutland Avenue, Baltimore, MD, United States.
E-mail address: awjames@jhmi.edu (A.W. James).
[1] The authors share equally in the work presented herein.

https://doi.org/10.1016/j.jor.2018.01.028
Received 20 August 2017; Accepted 14 January 2018
Available online 31 January 2018

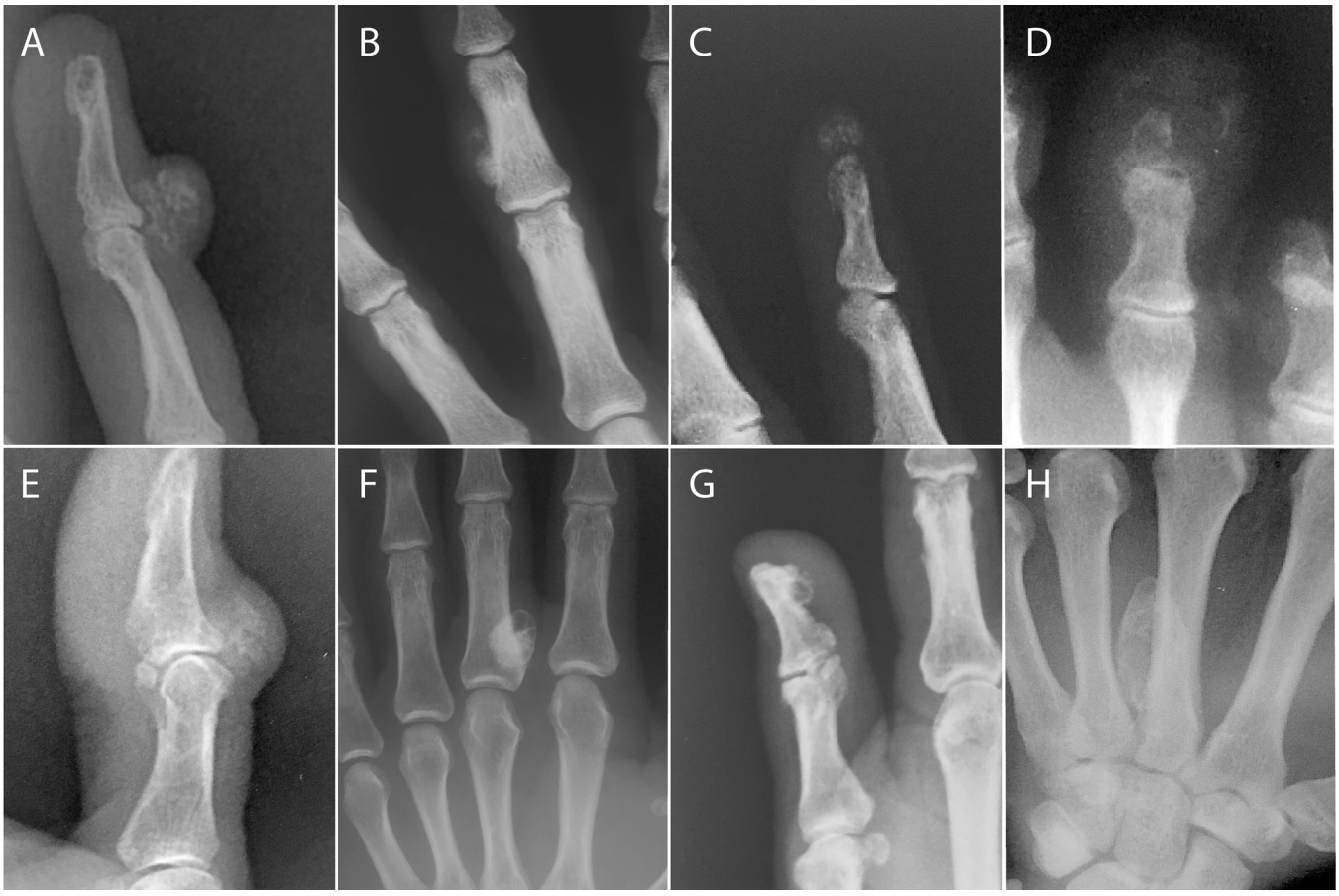

Fig. 1. Representative radiographic images of bizarre parosteal osteochondromatous proliferation. All were taken of the hands except for **D**, which is of the toes. **(A)** Dorsal multilobular radiodensity of the fourth distal phalanx with surrounding soft tissue prominence that has no apparent communication to the underlying bone marrow. **(B)** Parosteal radiodense mass adjacent to the middle phalanx of the third digit, appears to be a surface lesion. **(C)** Soft tissue mass with radiodensity distal to the distal phalanx. **(D)** Soft tissue mass with peripheral radiodensity that is associated with the distal phalanx, probably with periosteal reaction. Appearance of this lesion is less mature than in the prior examples. **(E)** Dorsal soft tissue lesion with internal radiodensity at the level of the interphalangeal joint of the thumb. Note similarity to radiograph in part **A**. **(F)** Radiodense mass at the proximal aspect of the proximal phalanx of the digit. From this view, possible attachment to the adjacent bone cortex cannot be excluded. **(G)** Volar surface lesion along the distal phalanx with peripheral radiodensity. **(H)** Large radiodense mass with smooth external border along the proximal metacarpal of the long finger with unclear relationship to the underlying bone.

2.3. Analysis of bizarre parosteal osteochondromatous proliferation samples

After digital slide imaging at 40× magnification, the percentage tissue composition of each sample was quantified using Adobe Photoshop based histomorphometry. Quantified areas of tissues included bone, cartilage, fibrous tissue and 'blue bone,' examined using two independent techniques. First, each tissue type with a distinct hue on H&E staining was quantified using the "magic wand tool" in Photoshop, selecting and counting pixels of a similar hue. Blue bone, cartilage, and bone tissue were quantified in this manner, and divided by the total number of pixels in the image to yield the percentage composition of each tissue type. Fibrous tissue was quantified using the "lasso" selection tool, as variability in hue precluded use of the magic wand tool (Supplemental Fig. 1). Again, the composition of fibrous tissue was calculated by dividing pixels of fibrous tissue by total pixel number in the image. Percentages were rounded to the nearest 5%. Tissue composition for each sample was compiled into graphs using GraphPad Prism (Fig. 3).

2.4. Statistical methods

Percent composition of tissue type for each sample was determined by histomorphometric analysis of representative 40 x images. Percentages summing to 100% for each sample are presented in a bar graph in Fig. 3**A**. Scatterplots in Fig. 3**B**–**E** organize the data by tissue type. Dots in the scatterplots represent individual samples, while sample mean and SEM are indicated by crosshairs and whiskers. Values are accurate to within 5%.

3. Results

3.1. Patient demographics

16 cases of BPOP were identified for inclusion. Five of the patients were female (5/16, 31%). Patients' ages ranged from 18 to 79, with six cases occurring between 20 and 40 years of age. 14 cases were located on the hands (14/16, 88%), 2 on the feet (2/16, 13%), 13/16 (81%) in the phalanges and 3/16 (19%) in the metacarpals. Of the tumors in the phalanges, 2/12 (17%) were located on the proximal phalanx, 7/12 (58%) on the distal phalanx and 3/12 (25%) on the middle phalanx. One case on the phalanx did not include specific location information (Supplemental Table 1).

3.2. Radiographic appearance

Available radiologic images are shown in Fig. 1. A radiodense mass was noted on or adjacent to the bone surface in all cases. Location was variable, with some lesions identified at the proximal phalanx (Fig. 1**G**), middle phalanx (Fig. 1**B**), distal phalanx (Fig. 1**C,D,F**), volar surface (Fig. 1**F**) or dorsal surface (Fig. 1**E**). No apparent communication to the underlying medullary cavity was identified in any instance. There was also a range of maturity of lesion, from predominant soft tissue swelling